

# On subthreshold solutions of the Hodgkin-Huxley equations

(action potential/nerve impulse propagation)

LAWRENCE SIROVICH\*† AND BRUCE W. KNIGHT\*

\* The Rockefeller University, New York, New York 10021; and † Brown University, Providence, Rhode Island 02912

Communicated by Floyd Ratliff, October 3, 1977

**ABSTRACT** Subthreshold solutions of the Hodgkin-Huxley equations are considered here by means of the linearized forms of these equations. An asymptotic theory is obtained, based on dimensional analysis and scaling arguments. Explicit expressions for the crest speed are obtained and are shown to be in good agreement with experiment, with computation, and with an exact asymptotic value which is also obtained here.

The firing of an impulse in a nerve requires that the membrane potential attain a threshold value. Experiment and computation based on the Hodgkin-Huxley (HH) equations (1) have shown that subthreshold responses appear as decremting waves that have a velocity close to that of the full nerve impulse (2). Because subthreshold potential excursions are relatively small, a linearized theory should be applicable. Indeed, a numerical integration of the linearized HH equations has been shown to agree with the comparable numerical integration of the full nonlinear HH equations (3). Because the linearized HH equations are essentially diffusive, whereas the velocity of the full impulse is due to nonlinear mechanisms, the analytical investigation of the linear problem is of mathematical as well as physical interest. In this report we outline an investigation of this problem that proceeds by means of scaling arguments and asymptotic analysis.

## Linearized equations and scaling

According to the theory of Hodgkin and Huxley (1, 4), the membrane potential ( $V$ ) is controlled by three currents: sodium, potassium, and leakage. The sodium current in turn is controlled by two kinetic variables, an activation variable  $m$ , and an inactivation variable  $h$ . Potassium current is controlled by the single kinetic variable  $n$ . The first step of a linear analysis is to assume that all four dependent variables of the HH equations are independent of both space and time. Set all derivatives equal to zero, and solve the four equations for their equilibrium or so-called resting values ( $V_0, m_0, h_0, n_0$ ). In what follows, we use the variables ( $V, m, h, n$ ) to denote the small departures of the HH variables from these resting values. The linearized HH equations then have the form:

$$\frac{\partial}{\partial t} V = a_{vv}V + a_{vm}m + a_{vh}h + a_{vn}n + \bar{G} \frac{\partial^2 V}{\partial x^2} \quad [1]$$

$$\frac{\partial m}{\partial t} = a_{mv}V + a_{mm}m \quad [2]$$

$$\frac{\partial h}{\partial t} = a_{hv}V + a_{hh}h \quad [3]$$

$$\frac{\partial n}{\partial t} = a_{nv}V + a_{nn}n. \quad [4]$$

We have used letter subscripts so that comparison with the

The costs of publication of this article were defrayed in part by the payment of page charges. This article must therefore be hereby marked "advertisement" in accordance with 18 U. S. C. §1734 solely to indicate this fact.

nonlinear equations (4) may be made easily. The coefficients that occur in the equations for the kinetic variables are dependent upon temperature and, at the reference temperature of 6.3°, to which we restrict attention here, assume the values:

$$\begin{aligned} a_{vv} &= -0.677354 & a_{vm} &= 69.1479 & a_{vh} &= 2.04667 & a_{vn} &= -55.3988 \\ a_{mv} &= 0.02637 & a_{mm} &= -4.22356 & & & & \\ a_{nv} &= -0.004107 & & & a_{hh} &= -0.117426 & & \\ a_{nv} &= 0.002806 & & & & & a_{nn} &= -0.183198. \end{aligned}$$

Customary practice has been followed: the units are millivolts, millimeters, and milliseconds. The perturbations  $m, h, n$  carry no dimensions and, by hypothesis, are assumed to be small compared to unity. An appropriate normalization for the perturbed membrane potential is

$$V = vV_0; V_0 = |a_{mm}|/a_{mv} \approx 160 \text{ mV}.$$

We introduce this normalization and rearrange terms somewhat to obtain Eqs. 1 and 2 in the form,

$$\begin{aligned} \frac{\partial v}{\partial t} &= \left( a_{vv} + \frac{a_{vm}}{V_0} \right) v + \frac{a_{vn}}{V_0} n + \bar{G} \frac{\partial^2 v}{\partial x^2} \\ &+ \left\{ \frac{a_{vm}}{V_0} (m - v) + \frac{a_{vh}}{V_0} h \right\} \quad [5] \\ \frac{1}{a_{mm}} \frac{\partial m}{\partial t} &= m - v. \end{aligned}$$

Here  $1/|a_{mm}|$ , the sodium turn-on time, is the fastest time scale of the problem and for  $t \gg 1/|a_{mm}|$ , the lower equation yields  $v \sim m$ . Therefore, from this and the smallness of  $a_{vh}/V_0$ , we may neglect the terms contained in the curly bracket of Eq. 5. Potassium activation,  $n$ , is then easily eliminated by means of Eq. 4, to give:

$$\begin{aligned} \left( \frac{\partial}{\partial t} - a_{nn} \right) \frac{\partial v}{\partial t} &= \left( a_{vv} + \frac{a_{vm}}{V_0} \right) \left( \frac{\partial}{\partial t} - a_{nn} \right) v \\ &+ a_{vn} a_{nv} v + \bar{G} \left( \frac{\partial}{\partial t} - a_{nn} \right) \frac{\partial^2 v}{\partial x^2}. \quad [6] \end{aligned}$$

Next, if we set

$$v = \varphi \exp(a_{nn}t),$$

the diffusion term in Eq. 6 is eliminated, whence

$$\frac{\partial^2 \varphi}{\partial t^2} = \left( a_{vv} - a_{nn} + \frac{a_{vm}}{V_0} \right) \frac{\partial \varphi}{\partial t} + a_{vn} a_{nv} \varphi + \bar{G} \frac{\partial^3 \varphi}{\partial x^2 \partial t}.$$

It now is natural to normalize  $t$  and  $x$  as follows:

$$\tau = \sqrt{-a_{vn} a_{nv}} t, \quad \chi = [-a_{vn} a_{nv} / \bar{G}^2]^{1/4} x \quad [7]$$

Abbreviation: HH, Hodgkin-Huxley.

which yields

$$L\varphi \equiv \frac{\partial^2 \varphi}{\partial t^2} + 2\lambda \frac{\partial \varphi}{\partial t} + \varphi - \frac{\partial^3 \varphi}{\partial t \partial \chi^2} = 0 \quad [8]$$

in which

$$\lambda = \frac{1}{2} (-a_{vv} + a_{nn} - a_{vm}/V_0) / \sqrt{-a_{nv}a_{vn}}. \quad [9]$$

Thus, the problem has been reduced to a third-order equation, Eq. 8, which has a single temperature-dependent parameter,  $\lambda$ . At the reference temperature  $\lambda(6.3^\circ) = 0.079$ . Because it is  $2\lambda \approx 0.16$  which enters into the equation, we will not neglect this term in what follows.

**Source and pulse solutions**

Both the experiments and the computations in ref. 2 consider a current source that is uniform in time and that is located at the origin. The wave velocity of the resulting response then may be determined by following the crest of the voltage displacement. An equivalent procedure is to consider a source that is a delta function both in space and in time and follow the first zero crossing of the response. This is the approach taken here; we consider

$$L\varphi = I^0 \delta'(\tau) \delta(\chi) \quad [10]$$

in which the value of the constant  $I^0$  is unimportant. (The derivative of the delta function appears on the right of Eq. 10 rather than the delta function, because of the various manipulations leading to this equation.) Because the current source is the only perturbation to the system, the initial value of  $(V; m, h, n)$  is zero. From this it follows that the initial values of  $\varphi$  and  $\varphi_t$ , which must enter into the solution of Eq. 10, are also zero, initially.

The solution to the problem just posed may be obtained by Laplace transform and a convenient form is

$$v = \frac{I^0}{16\pi i} \int_{\uparrow} \frac{\exp(\tau y - \chi \sqrt{y + 2\lambda + 1/y})}{\sqrt{y + 2\lambda + 1/y}} dy. \quad [11]$$

The path of integration lies to the right of the branch points of  $\sqrt{y + 2\lambda + 1/y}$  and, for large  $|y|$ , becomes asymptotic to the imaginary axis. We consider the first zero of  $v$  (corresponding to the crest locus of the steady current source problem) in two different limits.

**Asymptotic calculations**

Small  $\chi$ : If we set  $v$ , as given by Eq. 11, to zero and expand for  $\chi$  small, we obtain

$$0 = F_0(\tau) + \chi^2 F_1(\tau) + O(\chi^3) \quad [12]$$

in which

$$F_0 = \frac{\partial}{\partial \tau} \left[ \frac{1}{\tau} * (\exp -\lambda\tau) J_0(\tau\sqrt{1-\lambda^2}) \right]$$

$$F_2 = \frac{1}{2} \sqrt{1-\lambda^2} \left[ \frac{1}{\sqrt{\tau}} * \frac{(\exp -\lambda\tau) J_1(\tau\sqrt{1-\lambda^2})}{\tau} \right].$$

Here,  $J_0$  and  $J_1$  denote Bessel functions, and the asterisk indicates convolution. To solve for the zero locus, we express this trajectory in perturbation form:

$$\tau = \tau_0 + \chi^2 \tau_2 + O(\chi^3).$$

Then, from Eq. 12 we obtain

$$F_0(\tau_0) = 0$$

$$\tau_2 = -F_2(\tau_0)/F_0'(\tau_0).$$

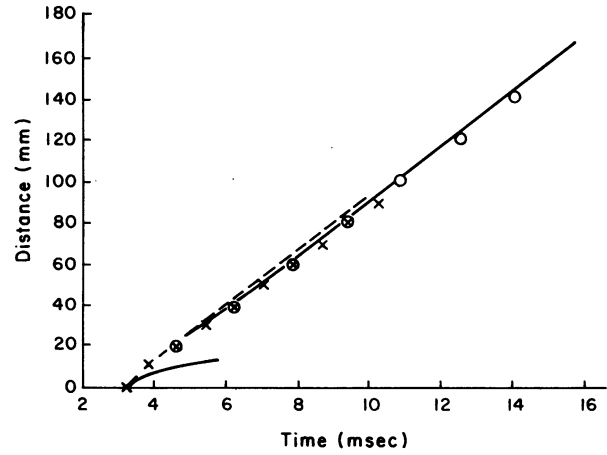


FIG. 1. Crest locus as a function of time (see text). (X), Numerical integration of HH equations; (O) numerical integration of linearized HH equations (J. W. Cooley, personal communication).

The first-order relationship,  $F_0(\tau_0) = 0$ , has an infinite number of positive roots, signifying oscillations; however, it is the first zero which corresponds to the observed crest. For the indicated value of  $\lambda$ , Eq. 9, we find

$$\tau_0 = 1.261, \quad \tau_2 = 0.4542.$$

In dimensional terms, the time of the first appearance of the crest (see Eq. 7) is given by

$$\tau_0 / \sqrt{-a_{nv}a_{vn}} \approx 3.198 \text{ msec.}$$

This compares with 3.315 msec found in ref. 2 from the numerical integration of the exact HH equations. (Note that this time is large compared to the sodium "turn-on" time  $1/|a_{mm}| \sim 0.2368$  msec, which fact underlines the basic correctness of the asymptotic procedure.)

A plot, in dimensional terms, of the small  $\chi$  locus is shown in Fig. 1. If we solve for  $\chi$  from the above we obtain

$$\chi = \sqrt{(\tau - \tau_0)/\tau_2} + O(\tau - \tau_0)$$

which implies an initial crest speed that is infinite. This feature is found also in experiment and in computation (2).

Large  $\tau$ : Set  $\chi = U\tau$ , whereupon Eq. 11 becomes

$$v = \frac{I^0}{16\pi i} \int_{\uparrow} \frac{\exp(\tau \mathcal{E}(y; U))}{\sqrt{y + 2\lambda + 1/y}} dy \quad [13]$$

with

$$\mathcal{E}(y; U) = y - U\sqrt{y + 2\lambda + 1/y}.$$

We now consider Eq. 13 for  $\tau \uparrow \infty$ . Under this limit, for any fixed  $U$ , the maximal contribution comes from the saddle point (5) which is obtained from the condition that the coefficient of  $\tau$  be stationary,  $(d\mathcal{E}/dy) = 0$ , which yields

$$\frac{1}{U} = \frac{1 - 1/y^2}{2\sqrt{y + 2\lambda + 1/y}}. \quad [14]$$

Fig. 2 contains a plot of the right hand side of Eq. 14. For  $U > U_{\max}$ , two real roots are possible; however, only a saddle point to the right of  $y_m$  is accessible.<sup>‡</sup> For  $U < U_{\max}$ , complex conjugate saddle point locations are obtained. Clearly, because  $y_m$  is a point of coalescence of two stationary points, the second

<sup>‡</sup> Evaluation by the saddle point method requires passage of the integration contour from a valley over a saddle point to an adjoining valley (5).

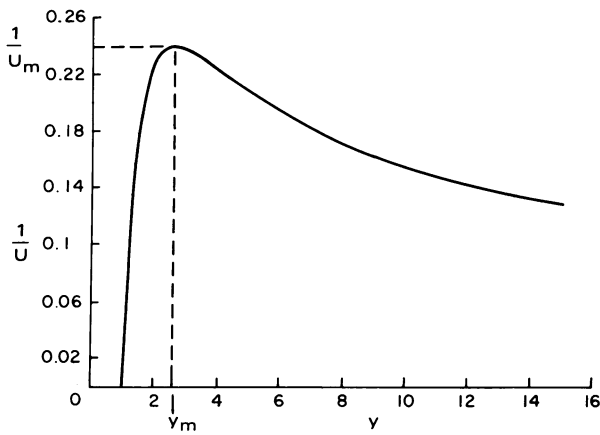


FIG. 2. Asymptotic saddle locus, Eq. 14 in dimensionless form.

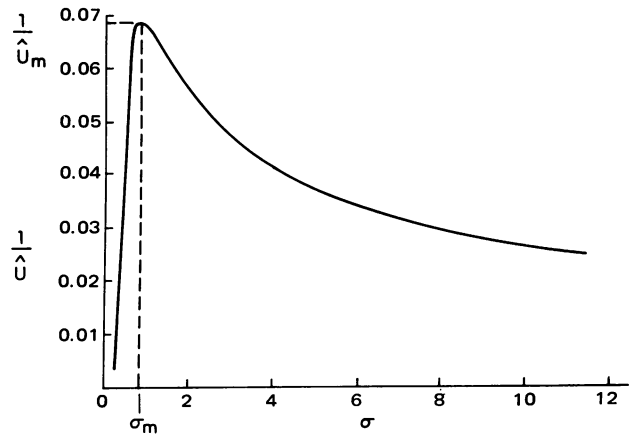


FIG. 3. Exact saddle locus (see text).

derivative of the exponent,  $\mathcal{E}$ , vanishes at this point.

On applying the saddle point method to Eq. 13, we find that  $v \neq 0$  for  $U > U_{max}$ . The first zero of  $v$  occurs when  $U$  lies in the neighborhood of  $U_{max}$ , and the resulting evaluation of  $U$  requires a stationary point analysis about the point  $y_m$ . If  $U = U_m$ , then at  $y_m$ , both the first and second derivatives of  $\mathcal{E}$  vanish—i.e., it is a “monkey saddle.”

To evaluate Eq. 13 in the neighborhood of  $y_m$ , we expand  $\mathcal{E}$  as follows:

$$\mathcal{E} \approx \mathcal{E}_m + \epsilon(y - y_m) + \frac{1}{3}c(y - y_m)^3$$

with

$$\begin{aligned} \mathcal{E}_m &= \mathcal{E}(y_m; U_m) \\ c &= 3U/(y_m - 1/y_m)U_m^3 \\ \epsilon &= 1 - U/U_m. \end{aligned}$$

If we substitute this into Eq. 13 we obtain

$$v \sim \frac{\exp(\mathcal{E}_m \tau)}{8(c\tau)^{1/3}} A_1(\epsilon\tau^{2/3}/c^{1/3}) \quad [15]$$

in which  $A_1$  is the Airy integral (6, 7). From tables of the Airy function (7), we find the first zero of the Airy function and from this the asymptotic crest locus

$$\chi \sim U_m \tau - 2.338\tau^{1/3}(3U_m/y_m - 1/y_m)^{1/3}. \quad [16]$$

A dimensional plot of Eq. 16 is shown in Fig. 1. The asymptotic speed is  $U_m = 4.1612$ , which in dimensional form is (see Eq. 7 for the normalization factor)

$$[\bar{G}^2 |a_{nv} a_{vn}|]^{1/4} U_m = 15.148 \text{ mm/msec}. \quad [17]$$

Before discussing these results further, we consider the exact asymptotic speed as given by the linearized Eqs. 1–4.

### Exact crest speed

We return to the linearized HH system, Eqs. 1–4. These may be solved by transform methods. For the case of a source pulse of current,  $I_0 \delta(x) \delta(t)$ , the solution for  $V$  is

$$V = \frac{I_0}{\bar{G} 4\pi i} \int_{\uparrow} \frac{\exp[\sigma - k(\sigma)\hat{U}]t}{k(\sigma)} d\sigma$$

with

$$k(\sigma) = \left( \sigma - a_{vv} - \frac{a_{mv} a_{vm}}{\sigma - a_{mm}} - \frac{a_{nv} a_{vn}}{\sigma - a_{nn}} - \frac{a_{hv} a_{vh}}{\sigma - a_{hh}} \right)^{1/2}$$

and  $x = \hat{U}t$  (note that we now are dealing with dimensional quantities). A saddle point argument similar to the previous one again applies. A plot of  $(dk/d\sigma)$  versus  $\sigma$  is shown in Fig. 3. The value of  $\hat{U}$  corresponding to the monkey saddle,  $y_m$ , is easily obtained and is given by

$$\hat{U}_m = 14.562 \text{ mm/msec}$$

which is to be compared with the asymptotic value given by Eq. 17.

### Discussion

The two asymptotic forms of the crest speed locus can be joined by resorting to an analysis based on the complex valued saddle points, when  $U < U_M$ . This results in the broken line sketched in Fig. 1. Our asymptotic analysis indicates that the crest speed, after an initial infinite value, falls below its asymptotic value, given by Eq. 17, and, as  $t \uparrow \infty$ , only very slowly, approaches its asymptote. This is indicated explicitly in the speed locus shown in Fig. 4 where the dashed curve refers to results of an approximate method. Although the paper by Mauro *et al.* (2) does not indicate this crest speed minimum, subsequent numerical calculations by J. W. Cooley (personal communication) based both on the nonlinear and linear HH equations show this feature. The results of Cooley’s calculations are indicated by symbols in Fig. 1. We have also used finite differences on these to calculate the speeds which are indicated by symbols in Fig. 4. In both figures, small and large  $x$  asymptotics are indicated by solid lines.

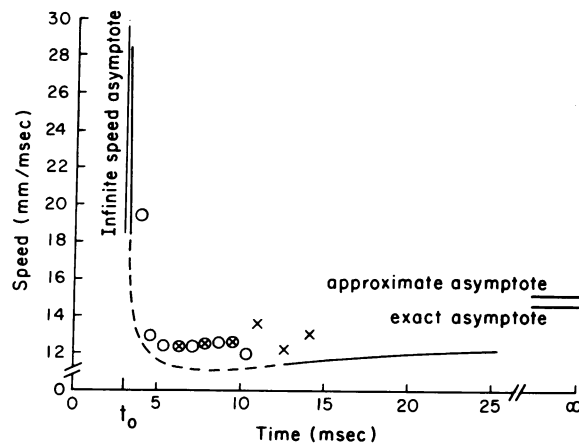


FIG. 4. Crest speed locus (see text and legend to Fig. 1).

In summary we have shown how simple approximation procedures, based upon general scaling arguments and upon asymptotic analysis, may be used to reduce the linearized HH equations to a simple model system that involves a single parameter. This model system yields tractably to a method of solution which, upon further asymptotic approximation, replicates, to within less than 10%, the locations of distinguished features found in the corresponding solution to the full HH system. A prominent feature that emerges naturally from the analysis is a decremting propagating wave.

Our method may be of some interest in connection with the subthreshold propagation of synaptic signals in dendritic trees.

The close numerical correspondence between the speed of the decremting wave and the speed of the full-sized action potential holds out the hope that salient features of the full nonlinear analysis as well may be found in this simple linear analysis.

We are grateful to Alex Mauro for bringing this problem to our attention. Also our deep gratitude to Jim Cooley for his kindness in sharing his results with us. This work was supported in part by Grants

EY 188, EY 1428, and EY 1472, from The National Eye Institute, National Institutes of Health.

1. Hodgkin, A. L. & Huxley, A. F. (1952) "A quantitative description of membrane current and its application to conduction and excitation in nerve," *J. Physiol. (London)* **117**, 500-544.
2. Mauro, A., Freeman, A. R., Cooley, J. W. & Cass, A. (1972) "Propagated subthreshold oscillatory response and classical electrotonic response of squid giant axon," *Biophysik* **8**, 118-132.
3. Sabah, N. H. & Leibovic, K. N. (1969) "Subthreshold oscillatory response of the Hodgkin-Huxley cable model for the squid giant axon," *Biophys. J.* **9**, 1206-1222.
4. Cooley, J. & Dodge, F. (1966) "Digital computer solutions for excitation and propagation of the nerve impulse," *Biophys. J.* **6**, 583-599.
5. Sirovich, L. (1971) *Techniques of Asymptotic Analysis* (Springer-Verlag, New York), pp. 105-134.
6. Magnus, W., Oberhettinger, F. & Soni, R. P. (1966) *Formulas and Theorems for the Special Functions of Mathematical Physics* (Springer-Verlag, New York), pp. 75-77.
7. Miller, J. C. P. (1946) *The Airy Integral, British Association for the Advancement of Science* (Cambridge University Press, Cambridge, England), Part-Vol. B (Math Tables).